44

Solute Dispersion Coefficients and Retardation Factors

M. Th. VAN GENUCHTEN

U.S. Salinity Laboratory, Agricultural Research Service, USDA Riverside, California

P. J. WIERENGA

New Mexico State University Las Cruces, New Mexico

44-1 INTRODUCTION

Modern agriculture uses substantial quantities of fertilizers, pesticides, and other chemicals that are beneficial only in the upper part of the soil profile. Translocation of these chemicals to the subsoil makes them not only unavailable for plant uptake, but also poses a threat to the quality of underlying groundwater systems. Chemicals dumped in waste disposal sites are also subject to translocation to groundwater, drains, or even surface streams. The same is true for radioactive materials and other chemicals spilled from waste storage reservoirs.

Various theoretical models have been developed over the years to describe chemical transport in soils. Success of these models depends to a large degree on our ability to quantify the transport parameters that enter into these models. Important parameters are the fluid flux, the dispersion coefficient, and the adsorption or exchange coefficients in case of interactions between the chemical and the solid phase. Simple linear adsorption or exchange can be accounted for by introducing a retardation factor in the transport equation. Various zero- or first-order production or decay coefficients may be required also (for example, when predicting transport of certain organic compounds, N species, or radionuclides).

A large number of methods are available for determining the dispersion coefficient and the retardation factor from observed solute concentration distributions. This chapter describes five different techniques that are applicable to both laboratory and field displacement experiments. A few other methods exist that, in addition to those discussed here, can also be used to obtain estimates for the dispersion coefficient and the retardation factor. They include the method of moments (Aris, 1958;

Agneessens et al., 1978; Skopp, 1985; Valocchi, 1985; Jury & Sposito, 1985; among others), and methods to determine the two coefficients from the location and peak concentration of a short or instantaneous surface-applied tracer pulse (Kirkham & Powers, 1972; Saxena et al., 1974; Yu et al., 1984). The reader is referred to the original studies for a discussion of these additional methods.

44-2 THEORETICAL PRINCIPLES

All available methods for determining the required transport parameters from observed concentration distributions are based on analytical solutions of the solute transport equation. Consequently, we will first give a brief discussion of the transport equation and of various boundary conditions that have been used to derive analytical solutions of that equation.

44-2.1 Transport Equation

Consider the situation where water containing a dissolved tracer is applied to a tracer-free soil profile. As more of the solution is added, the initially very sharp tracer front near the soil surface becomes more and more spread out (dispersed) due to the combined effects of diffusion and convection. Transport of the dissolved tracer consists of three components:

Convective or Mass Transport (J_m). Convective (or advective) transport refers to the passive movement of the dissolved tracer with flowing soil water. In the absence of diffusion, water and the dissolved tracer move at the same average rate

$$J_m = q\,C \qquad\qquad [1]$$

where q is the volumetric fluid flux density and C is the volume-averaged solute concentration.

Diffusive Transport (J_D). Diffusion is a spontaneous process that results from the natural thermal motion of dissolved ions and molecules. Diffusive transport in soils tends to decrease existing concentration gradients, and in analogy to Fick's law, can be described by

$$J_D = -\theta D_m \frac{\partial C}{\partial x} \qquad\qquad [2]$$

where θ is the volumetric water content, D_m is the porous medium ionic or molecular diffusion coefficient, and x is distance. Because of a tortuous flow path, D_m in soils is somewhat less than the diffusion coefficient in pure water (D_o):

$$D_m = D_o \tau \qquad\qquad [3]$$

where τ is a dimensionless tortuosity factor, ranging roughly from 0.3 to about 0.7 for most soils.

Dispersive Transport (J_h). Dispersive transport results from the fact that local fluid velocities inside individual pores and between pores of different shapes, sizes, and directions, deviate from the average pore-water velocity. Such velocity variations cause the solute to be transported down-gradient at different rates, thus leading to a mixing process that is macroscopically similar to mixing caused by molecular diffusion. Dispersion is a passive process that, unlike diffusion, occurs only during water movement. On the other hand, diffusion always forms an integral part of the overall dispersion process by reducing flow-induced concentration gradients within and between pores. Because of the passive nature of the dispersion process, the term *mechanical dispersion* is often used to describe mixing caused by local velocity variations (Fried & Combarnous, 1971; Bear, 1972; Freeze & Cherry, 1979). Laboratory and field experiments have shown that dispersive transport can be described by an equation similar to Eq. [2] for diffusion

$$J_h = -\theta D_h \frac{\partial C}{\partial x} \tag{4}$$

where D_h is the mechanical dispersion coefficient (Bear, 1972). This coefficient is generally assumed to be a function of the fluid velocity

$$D_h = \lambda v^n \tag{5}$$

where λ is the dispersivity and v the average interstitial or pore-water velocity, approximated by the ratio q/θ. The exponent n in Eq. [5] is an empirical constant, roughly equal to 1.0. For most laboratory displacement experiments involving disturbed (repacked) soils and for certain uniform field soils, λ is on the order of about 1 cm or less (assuming that $n = 1$). For transport problems involving undisturbed field soils, especially when aggregated, λ is usually about one or two orders of magnitude larger.

Because of the macroscopic similarity between molecular diffusion and mechanical dispersion, the coefficients D_m and D_h are often considered additive

$$D = D_m + D_h \tag{6}$$

where D is the longitudinal hydrodynamic dispersion coefficient (Bear, 1972), further referred to simply as the dispersion coefficient. Other terms frequently used for D are the *apparent diffusion coefficient* (Nielsen et al., 1972; Boast, 1973), and the *diffusion-dispersion coefficient* (Hillel, 1980), while the term *hydrodynamic dispersion coefficient* sometimes has been reserved for D_h only (Shamir & Harleman, 1966; Nielsen et al., 1972; Boast, 1973).

Combining Eq. [1], [2], [4], and [6] leads to the following expression for the solute flux, J_s:

$$J_s = - \theta D \frac{\partial C}{\partial x} + qC.$$ [7]

Substituting Eq. [7] into the equation of continuity

$$\frac{\partial}{\partial t}(\theta C + \rho S) = - \frac{\partial J_s}{\partial x}$$ [8]

yields the transport equation

$$\frac{\partial}{\partial t}(\theta C + \rho S) = \frac{\partial}{\partial x}\left(\theta D \frac{\partial C}{\partial x} - qC\right)$$ [9]

where S is the adsorbed concentration (mass of solute per unit mass of soil), ρ is the soil bulk density, and t is time. The two terms on the left side of Eq. [9] account for changes in solute concentrations associated with the liquid and solid phases, respectively.

We assume here that S and C can be related by a linear or linearized equilibrium isotherm of the form

$$S = kC$$ [10]

where k is an empirical distribution coefficient. The assumption of linear adsorption generally is valid only at low concentrations. Note that Eq. [9] assumes that the chemical is not subject to any production or decay processes. A few comments about the determination of zero- and first-order production or decay coefficients from observed displacement experiments are given in section 44-9.

If, in addition to linearized equilibrium adsorption, steady water flow in a homogeneous soil profile is assumed (θ and q are constant in time and space), Eq. [9] reduces to

$$R \frac{\partial C}{\partial t} = D \frac{\partial^2 C}{\partial x^2} - v \frac{\partial C}{\partial x}$$ [11]

where R is the retardation factor

$$R = 1 + \rho k/\theta.$$ [12]

If there are no interactions between the chemical and the soil, k becomes zero and R reduces to one. In some cases R may become less than one, indicating that only a fraction of the liquid phase participates in the transport process. This may be the case when the chemical is subject to anion exclusion or when relatively immobile liquid regions are present,

for example inside dense aggregates, that do not contribute to convective transport. In case of anion exclusion, $(1-R)$ may be viewed as the relative anion exclusion volume.

44-2.2 Boundary Conditions and Analytical Solutions

To complete the mathematical description of transport through semi-infinite field profiles $(0 \leqslant x < \infty)$ or finite laboratory columns of length L $(0 \leqslant x \leqslant L)$, Eq. [11] must be augmented with auxiliary conditions describing the initial concentration of the system and the boundary conditions. Proper formulation of the boundary conditions is important when analyzing laboratory displacement experiments involving relatively short columns, as well as for interpreting tracer data from laboratory or field profiles exhibiting large dispersivities λ. Also, incorrect use of boundary conditions for laboratory tracer experiments can lead to serious errors when the experimental results subsequently are extrapolated to field situations.

Table 44–1 summarizes four available analytical solutions of Eq. [11] for both semi-infinite (A-1, A-2) and finite systems (A-3, A-4). The analytical expressions hold for the relative concentration c, which is defined as

$$c(x,t) = [C(x,t) - C_i]/(C_o - C_i) \qquad [13]$$

where C_o is the concentration of the applied solution and C_i the initial concentration. Both C_i and C_o are assumed to be constant.

When a tracer solution is applied at a specified rate from a perfectly mixed inlet reservoir to the surface of a finite or semi-infinite soil profile, continuity of the solute flux across the inlet boundary leads directly to a third-type or flux-type boundary condition of the form

$$\left(-D \frac{\partial C}{\partial x} + vC \right) \Bigg|_{x=0+} = vC_o \qquad [14]$$

where $0+$ indicates evaluation at the inlet boundary just inside the medium.

For semi-infinite systems in the field we also need a boundary condition that specifies the behavior of $C(x,t)$ when $x \to \infty$. For our discussion it is sufficient to require that

$$\frac{\partial C}{\partial x}(\infty, t) = 0. \qquad [15]$$

The analytical solution for boundary conditions [14] and [15] is given by case A-2 in Table 44–1. This solution correctly evaluates volume-averaged, in situ or resident concentrations in semi-infinite field profiles. For example, one may verify that solution A-2 satisfies the mass balance requirement

Table 44–1. Analytical solutions of Eq. [11] for various boundary conditions.

Case	Inlet boundary condition	Exit boundary condition	Analytical solution
A-1	$C(0, t) = C_o$	$\dfrac{\partial C}{\partial x}(\infty, t) = 0$	$c = \dfrac{1}{2}\,\text{erfc}\left[\dfrac{Rx - vt}{2(DRt)^{1/2}}\right] + \dfrac{1}{2}\exp\left(\dfrac{vx}{D}\right)\text{erfc}\left[\dfrac{Rx - vt}{2(DRt)^{1/2}}\right]$
A-2	$\left(-D\dfrac{\partial C}{\partial x} + vC\right)\Big|_{x=0} = vC_o$	$\dfrac{\partial C}{\partial x}(\infty, t) = 0$	$c = \dfrac{1}{2}\,\text{erfc}\left[\dfrac{Rx - vt}{2(DRt)^{1/2}}\right] + \left(\dfrac{v^2 t}{\pi DR}\right)^{1/2}\exp\left[-\dfrac{(Rx - vt)^2}{4DRt}\right] - \dfrac{1}{2}\left(1 + \dfrac{vx}{D} + \dfrac{v^2 t}{DR}\right)\exp\left(\dfrac{vx}{D}\right)\text{erfc}\left[\dfrac{Rx + vt}{2(DRt)^{1/2}}\right]$
A-3	$C(0, t) = C_o$	$\dfrac{\partial C}{\partial x}(L, t) = 0$	$c = 1 - \displaystyle\sum_{m=1}^{\infty} \dfrac{2\beta_m \sin\left(\dfrac{\beta_m x}{L}\right)}{\beta_m^2 + \left(\dfrac{vL}{2D}\right)^2 + \dfrac{vL}{2D}}\exp\left[\dfrac{vx}{2D} - \dfrac{v^2 t}{4DR} - \dfrac{\beta_m^2 Dt}{L^2 R}\right]$ $\beta_m \cot(\beta_m) + \dfrac{vL}{2D} = 0$
A-4	$\left(-D\dfrac{\partial C}{\partial x} + vC\right)\Big|_{x=0} = vC_o$	$\dfrac{\partial C}{\partial x}(L, t) = 0$	$c = 1 - \displaystyle\sum_{m=1}^{\infty} \dfrac{\dfrac{2vL}{D}\,\beta_m\left[\beta_m\cos\left(\dfrac{\beta_m x}{L}\right) + \dfrac{vL}{2D}\sin\left(\dfrac{\beta_m x}{L}\right)\right]\exp\left[\dfrac{vx}{2D} - \dfrac{v^2 t}{4DR} - \dfrac{\beta_m^2 Dt}{L^2 R}\right]}{\left[\beta_m^2 + \left(\dfrac{vL}{2D}\right)^2 + \dfrac{vL}{D}\right]\left[\beta_m^2 + \left(\dfrac{vL}{2D}\right)^2\right]}$ $\beta_m \cot(\beta_m) - \dfrac{\beta_m^2 D}{vL} + \dfrac{vL}{4D} = 0$

References: A-1: Lapidus and Amundson (1952)　　A-3: Cleary and Adrian (1973)
　　　　　　A-2: Lindstrom et al. (1967)　　A-4: Brenner (1962)

$$vC_ot = R\int_0^\infty \left[C(x,t) - C_i \right] dx. \qquad [16]$$

In other words, whatever material is added at the surface (term on the left) should be present in the soil profile (term on the right).

Instead of Eq. [14], a first- or concentration-type input boundary condition has also been used

$$C(0,t) = C_o. \qquad [17]$$

This equation assumes that the concentration itself can be specified at the inlet boundary, a situation that usually is not possible in practice. Analytical solution A-1 for this condition (see Table 44–1) fails to satisfy mass balance Eq. [16], the largest errors occurring at relatively small values of the dimensionless group v^2t/DR (van Genuchten & Parker, 1984). Hence, this solution should not be used for evaluating volume-averaged concentrations in semi-infinite field profiles. On the other hand, solution A-1 is useful for estimating solute fluxes at any point in the profile. As shown by Brigham (1974), Kreft and Zuber (1978), and Parker and van Genuchten (1984a), among others, solutions A-1 and A-2 are related through the transformation

$$C_f = C - \frac{D}{v}\frac{\partial C}{\partial x} \qquad [18]$$

where C_f, to be identified with analytical solution A-1, represents flux-averaged or flowing concentrations, in contrast to C (solution A-2), which represents volume-averaged or resident concentrations. In other words, the solute flux J_s (Eq. [7]) at any point in the profile is directly specified by $J_s = qC_f$ with C_f given by solution A-1.

Proper formulation of the exit boundary condition for displacement through finite laboratory columns is considerably more difficult than for semi-infinite field profiles. In analogy with Eq. [14], mass conservation requires the solute velocity to be continuous across the exit boundary

$$\left(-D\frac{\partial C}{\partial x} + vC \right)\Bigg|_{x=L-} = vC_e \qquad [19]$$

where $L-$ indicates evaluation just inside the column, and where C_e is the effluent concentration. This equation assumes negligible dispersion in the exit reservoir (or after-section). Because of an extra unknown (C_e), Eq. [19] leads to an indeterminate system of equations; hence, an additional relation is needed to fully describe the system. One such equation is based on the intuitive assumption that the concentration should be continuous at $x = L$:

$$C(L-, t) = C_e(t). \qquad [20]$$

Substitution of this equation into Eq. [19] leads to the frequently used boundary condition (Danckwerts, 1953)

$$\frac{\partial C}{\partial x}(L,t) = 0. \tag{21}$$

The analytical solution for boundary conditions [14] and [21], derived by Brenner (1962), is given by case A-4 in Table 44–1. Brenner's solution describes volume-averaged concentrations inside the column. Because of the zero concentration gradient at $x = L$, this solution also defines a flux concentration (Eq. [18]) at the lower boundary. Hence, Brenner's solution correctly interprets effluent concentrations as representing flux-averaged concentrations. Table 44–2 (case A-4) shows the resulting expression for the relative effluent concentration in terms of the number of pore volumes, T, leached through the column and the column Peclet number, P

$$T = vt/L \tag{22a}$$

$$P = vL/D. \tag{22b}$$

Computational programs for evaluation of Brenner's series solution are readily available (van Genuchten & Alves, 1982). The series solution converges only for relatively small values of P. For large P-values, computationally efficient and very accurate approximate solutions have also been obtained (van Genuchten & Alves, 1982).

Analogous to Eq. [16] for semi-infinite systems, the mass balance requirement for finite columns is

$$v \int_0^t \left[C_o - C_e(\tau) \right] d\tau = R \int_0^L \left[C(x,t) - C_i \right] dx. \tag{23}$$

This equation states that whatever is added to the column minus whatever is leaving that column (left side) must be stored in the column (right side). Upon substitution, it is easily demonstrated that solution A-4 satisfies Eq. [23]. Tables 44–1 and 44–2 also list analytical solution A-3 for boundary conditions [17] and [21]. Contrary to A-1 and A-2, solutions A-3 and A-4 are not related through the transformation given by Eq. [18]. Moreover, solution A-3 fails the mass-balance requirement (Eq. [23]), and as will be shown later, also violates a mass balance for the effluent curve. Hence, this solution should never be applied to displacement experiments.

The analysis above shows that Brenner's solution A-4 is based on the assumption that the concentration is continuous at $x = L$. An alternative formulation is possible by assuming that solute distributions inside the column are not affected by an outflow boundary or effluent collection system, thus considering the column to be part of an effectively

Table 44–2. Expressions for the relative effluent concentration, $c_e(T)$, in terms of the column Peclet number (P) and pore volume (T) for the four analytical solutions listed in Table 44–1.

Case	Relative effluent concentration
A-1	$c_e(T) = \dfrac{1}{2}\operatorname{erfc}\left[\left(\dfrac{P}{4RT}\right)^{1/2}(R-T)\right] + \dfrac{1}{2}\exp(P)\operatorname{erfc}\left[\left(\dfrac{P}{4RT}\right)^{1/2}(R+T)\right]$
A-2	$c_e(T) = \dfrac{1}{2}\operatorname{erfc}\left[\left(\dfrac{P}{4RT}\right)^{1/2}(R-T)\right] + \left(\dfrac{PT}{\pi R}\right)^{1/2}\exp\left[-\dfrac{P}{4RT}(R-T)^2\right] - \dfrac{1}{2}\left(1+P+\dfrac{PT}{R}\right)\operatorname{erfc}\left[\left(\dfrac{P}{4RT}\right)^{1/2}(R+T)\right]$
A-3	$c_e(T) = 1 - \displaystyle\sum_{m=1}^{\infty}\dfrac{2\,\beta_m\sin(\beta_m)\exp\left[\dfrac{P}{2}-\dfrac{PT}{4R}-\dfrac{\beta_m^2 T}{PR}\right]}{\beta_m^2 + \dfrac{P^2}{4} + \dfrac{P}{2}}$ $\beta_m\cot(\beta_m) + \dfrac{P}{2} = 0$
A-4	$c_e(T) = 1 - \displaystyle\sum_{m=1}^{\infty}\dfrac{2\,\beta_m\sin(\beta_m)\exp\left[\dfrac{P}{2}-\dfrac{PT}{4R}-\dfrac{\beta_m^2 T}{PR}\right]}{\beta_m^2 + \dfrac{P^2}{4} + P}$ $P\beta_m\cot(\beta_m) - \beta_m^2 + \dfrac{P^2}{4} = 0$

semi-infinite system. This in turn suggests that analytical solution A-2 of Table 44–1 adequately describes volume-averaged concentrations inside the column. Substituting this solution into Eq. [19] leads then to a different expression for the relative effluent concentration

$$c_e(t) = \frac{1}{2}\,\mathrm{erfc}\left[\frac{RL - vt}{2(DRt)^{1/2}}\right] + \frac{1}{2}\exp\left(\frac{vL}{D}\right)\mathrm{erfc}\left[\frac{RL + vt}{2(DRt)^{1/2}}\right] \quad [24]$$

which is the same as solution A-1 of Table 44–1, evaluated at $x = L$. This result is consistent with the notion that effluent concentrations are flux-averaged concentrations (Van Genuchten & Parker, 1984; Parker & Van Genuchten, 1984a). Hence, solution A-1 of Table 44–2 correctly predicts effluent curves from finite columns, given the assumption that the exit boundary does not affect transport inside the column.

To appreciate the effects of various boundary conditions, Fig. 44–1 shows, for three different values of P, calculated effluent curves based on the four analytical solutions listed in Table 44–2. Note that the solutions deviate drastically when $P = 1$, but slowly converge when P increases. Solutions A-1 and A-4 are similar when $P = 5$ and essentially identical when $P = 20$.

An important attribute of a breakthrough curve from a finite column is the area above each curve. This area, sometimes referred to as the
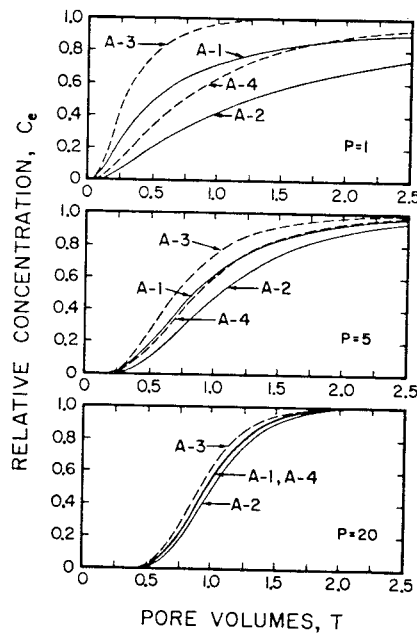

Fig. 44–1. Relative effluent concentration profiles for analytical solutions A-1 (Lapidus & Amundson, 1952), A-2 (Lindstrom et al., 1967), A-3 (Cleary & Adrian, 1973) and A-4 (Brenner, 1962). The effluent curves are plotted for three values of the column Peclet number, P.

holdup (H), represents the amount of material that can be stored in the column. Mathematically, H is given by

$$H = \int_0^\infty \left[1 - c_e(T) \right] dT. \qquad [25]$$

One may verify that $H = R$ for solutions A-1 and A-4. For solution A-2, H is given by (van Genuchten & Parker, 1984)

$$H = R[1 + (1/P)] \qquad [26]$$

while for solution A-3

$$H = R[1 - (1/P) + (e^{-P}/P)] . \qquad [27]$$

Figure 44-2 gives a plot of the relative holdup (H/R) vs. P for the four analytical solutions. Note that H/R deviates substantially from unity for solutions A-2 and A-3. Hence, highly inaccurate estimates for R can be obtained when these two solutions are fitted to column effluent data, especially when P is small. For example, solution A-2 overestimates R by about 50% when $P = 2$.

In conclusion, only solutions A-1 and A-4 for the effluent curve lead to correct estimates for R, irrespective of the value of P. However, these two solutions may yield slightly different estimates for P, especially when P is less than about 5 (Fig. 44-1). As pointed out before, solutions A-1 and A-4 are based on different assumptions regarding the physics of flow and transport at or near the lower boundary. Because of some inconsistencies in the stipulation of concentration continuities at the inlet and outlet boundaries for Brenner's solution (van Genuchten & Parker, 1984) and because of its numerically more tedious form compared to A-1, we recommend that solution A-1 always be used to calculate flux-averaged concentrations. whether they pertain to finite systems (effluent curves) or semi-infinite field profiles. We similarly recommend that solution A-2 always be used for volume-averaged resident concentrations.
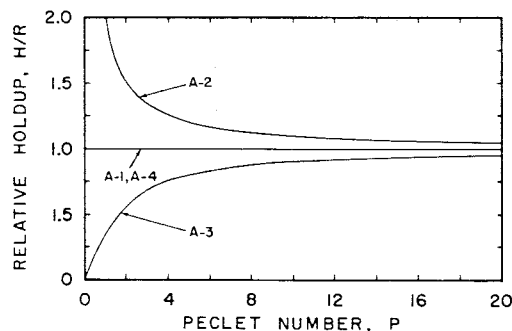

Fig. 44-2. Relative holdup (H/R) vs. column Peclet number (P) for the four analytical solutions of Table 44-2 (see also Fig. 44-1).

In some cases, breakthrough curves are obtained within laboratory columns by means of suction cups or other extraction devices. In that case, it is difficult to reason exactly which concentration mode will be observed. Because the soil solution is extracted at a fixed location in the soil, it is unlikely that the observed concentrations are flux concentrations. However, because of the transient behavior of displacement experiments and the uncertainty of how exactly flow lines are disrupted by the installation and performance of suction cups, observed concentrations are probably not exactly those of resident concentrations either. This problem is not only pertinent for laboratory experiments but also for in situ field measurements.

An expression not listed in Tables 44-1 or 44-2 but frequently used to describe displacement experiments is (Danckwerts, 1953; Rifai et al., 1956)

$$c(x,t) = \frac{1}{2} \mathrm{erfc}\left[\frac{Rx - vt}{2(DRt)^{1/2}} \right]$$ [28]

This equation provides a close approximation of the four analytical solutions in Table 44-1 for relatively large values of P. For example, Eq. [28] follows from solutions A-1 and A-2 by retaining only the first term of the analytical expressions. Equation [28] can be derived also from Eq. [11] by assuming either an infinite system ($-\infty < x < \infty$) or a purely dispersive system in which molecular diffusion is neglected (Rifai et al., 1956; Kirkham & Powers, 1972). Even though Eq. [28] is formally not applicable to either laboratory or field experiments, its simple form and the fact that the equation provides a close approximation of the analytical solutions when P is large makes it an attractive tool for deriving simple and approximate expressions for D in terms of measurable parameters.

44-3 EXPERIMENTAL PRINCIPLES

44-3.1 Special Apparatus

The apparatus for determining D and R consists of a precision constant-volume pump, a soil column, and a fraction collector (Wierenga et al., 1975) (Fig. 44-3). For unsaturated flow experiments, controlled vacuum is necessary, as well as a vacuum container to house the fraction collector. Columns for holding the soil are most conveniently constructed from plexiglass. Construction details are available from the second author.

The lower end of the plexiglass column has a bottom plate with an O-ring closely fitted inside the column. The top part of the bottom plate contains a fritted glass porous plate with a slightly smaller diameter. Space below the fritted glass plate and a hole in the center of the bottom plate
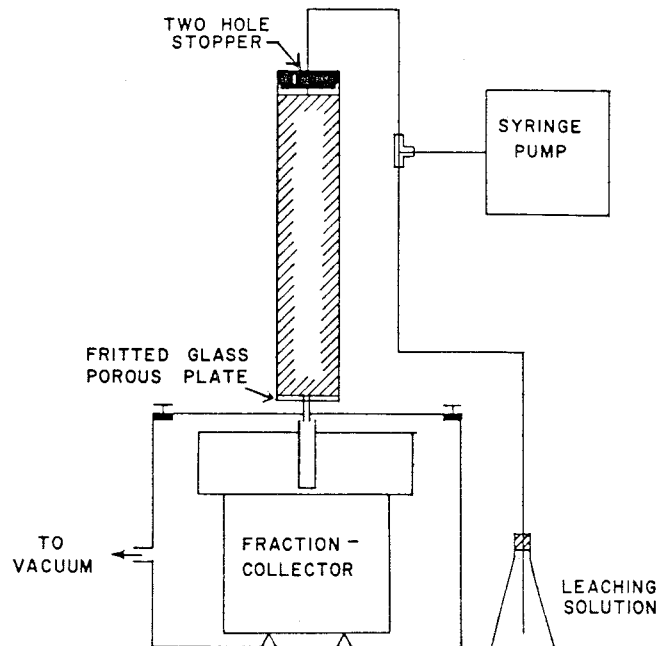
Fig. 44–3. Schematic diagram of experimental apparatus for column displacement experiments.

allow for drainage from the column. To reduce mixing in the end-plate assembly, it is important to keep the pore space of the end assembly as small as possible. For ions that react with fritted glass, stainless steel porous plates (Michigan Dynamics, Garden City, MI 48135) may be used. Unfortunately, these plates generally have a lower air-entry value than fritted glass plates. Alternatively, silver membranes (Selas Flotronics, Huntingdon Valley, PA 19006) may be used. They should be placed on top of the stainless steel plate or other coarse, porous material for support. Silver membranes have a high air-entry value and a low resistance to water flow. They are also very thin (0.5 mm) and thus contain minimal pore-space volume. At the upper end of the vertically placed soil column, the tracer solution can be applied through a porous plate or by means of an assembly of hypodermic needles (Gaudet et al., 1977) that spreads the solution evenly over the soil surface.

The column is placed above the fraction collector to collect the effluent in small-volume fractions. For unsaturated flow experiments, the fraction collector is placed inside a vacuum container which is connected to a vacuum supply by means of a vacuum regulator (Moore Products Co., Spring House, PA 19477). By locating the column outlet through a hole in the plexiglass cover of the container, a constant vacuum will be maintained at the lower end of the column. The magnitude of the required vacuum depends on the rate at which the solution is applied to the top of the column, and the hydraulic properties of the soil inside the column.

Ideally, the vacuum should be such that unit gradient flow conditions and a uniform water content distribution with depth exist within the column during the experiment. Constant flow conditions are best maintained by applying the solution with a precision constant-volume pump. Maintaining constant flow conditions is particularly important for experiments of long duration. When several columns are leached simultaneously, a multichannel syringe pump as described by Wierenga et al. (1973) may be considered. Where maintaining constant-flow conditions is less critical, or when the soil is to be maintained close to saturation, burettes may be used to apply the solution to the columns (Nielsen & Biggar, 1961). Although burettes make it more difficult to maintain constant-flux conditions, they do allow for a much better control of the pressure-head gradient inside the soil columns. With either pumps or burettes, it is important to be able to switch rapidly from one solution to another, with minimal mixing between the applied solutions in the inlet assembly.

44–3.2 Experimental Procedure

Upon collecting effluent samples, determining their concentration by standard chemical procedures, and plotting these concentrations vs. either time, volume of effluent ($V = Aqt$), or pore volume (T), an effluent curve is obtained. The number of pore volumes is calculated by dividing the amount of water leached through the column (V) by the liquid capacity ($V_o = A\theta L$) of the column

$$T = V/V_o = vt/L \qquad\qquad [29]$$

where L is the length and A the cross-sectional area of the column. The analysis of effluent curves is greatly facilitated by plotting relative concentrations (Eq. [13]) vs. pore volumes. Figure 44–4 shows typical effluent curves for the movement of tritiated water (^3H_2O) through a 30-cm long soil column and for chromium (Cr^{6+}) transport through a 5-cm long column of sand. Relevant data for these and two other experiments are listed in the appendix. The ^3H_2O-data are hypothetical insofar as they were calculated with solution A-1 (Table 44–2), with $R = 1$ and $P = 30$; the chromium data were actually measured. Both sets of data will be used in later sections to check the accuracy of the different methods.

We emphasize here that use of the dimensionless parameters P and T does not suggest that the different methods below are restricted only to finite laboratory soil columns. The parameter L in case of field-measured concentration-time curves simply refers to the soil depth at which the concentrations were observed. Hence, the methods below apply also to semi-infinite field profiles, provided that only methods based on solution A-2 (Tables 44–1 and 44–2) be used to estimate P and R from
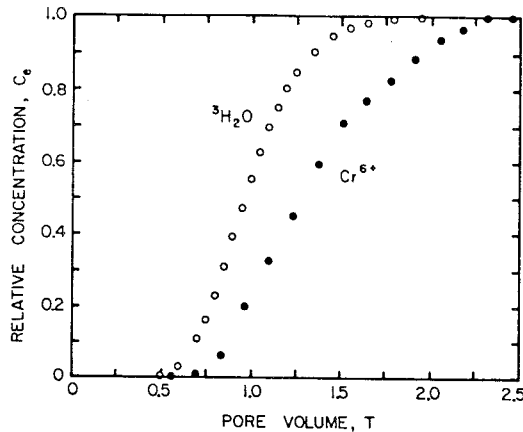
Fig. 44–4. Effluent curves for tritiated water ($^{3}H_2O$) and chromium (Cr^{6+}).

volume-averaged field concentration data. Once P is determined with whatever method, the value of D follows immediately from Eq. [22b].

44–4 METHOD I: TRIAL AND ERROR

44–4.1 Principles, Procedure, and Example

Estimates for P and R can be obtained by comparing the experimental curve directly with a series of calculated distributions and selecting those values of P and R that provide the best fit with one of the theoretical curves. An approximate estimate for R can be obtained first by locating the number of pore volumes ($T = R$) at which the relative concentration of the observed curve reaches 0.5. This property is based on Eq. [28], which at $x = L$ and in terms of P and T reduces to

$$c_r(T) = \tfrac{1}{2}\,\text{erfc}[(P/4RT)^{1/2}\,(R - T)]\,. \qquad [30]$$

Because $\text{erfc}(0) = 1$, it follows from Eq. [30] that $c_r(R) = 0.5$. As an example, Fig. 44–5 compares the $^{3}H_2O$-curve of Fig. 44–4 with theoretical curves based on solution A-1 of Table 44–2, using $R = 1$ and various values of P. Inspection of this figure shows that the correct value of P should be about 30 to 40.

44–4.2 Comments

From Fig. 44–5, it must be clear that trial-and-error methods can be cumbersome and time-consuming, and that they yield estimates for P and R that are not necessarily reproducible by two different investigators or by the same investigator on two different occasions.
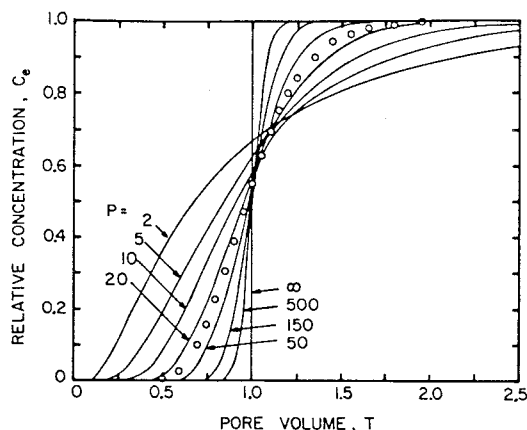
Fig. 44-5. Calculated effluent curves based on analytical solution A-1 (Table 44-2) and for various values of the column Peclet number, P. The "observed" curve (open circles) was obtained with $R = 1$ and $P = 30$.

44-5 METHOD II: FROM THE SLOPE OF AN EFFLUENT CURVE

44-5.1 Principles

Consider first the approximation given by Eq. [30] for the relative effluent concentration. Differentiation of this equation with respect to T, evaluating the resulting equation at $T = R$, and solving for P yields (see also Rifai et al., 1956)

$$P = 4\pi R^2 S_T^2 \qquad [31]$$

where S_T is the slope of the effluent curve after exactly R pore volumes. The retardation factor, R, again can be estimated by locating the value of T at which the relative concentration equals 0.5.

The method above is based on Eq. [30] and hence can give only approximate estimates for P and R. However, a similar method can also be derived from analytical solution A-1 of Table 44-2. Differentiation of that solution with respect to T and solving for P at $T = R$ also leads to Eq. [31]. Contrary to Eq. [30], however, solution A-1 does not yield a value of 0.5 after R pore volumes. This is shown in Fig. 44-6, where relative effluent concentrations at $T = R$, i.e., $c_e(R)$, are plotted vs. P for the four analytical solutions of Table 44-2. Note that $c_e(R)$ for case A-1 is always > 0.5, especially when P is small. Once approximate values of P and R are obtained by means of Eq. [31] and the initial assumption that $c_e(R) = 0.5$, curve A-1 of Fig. 44-6 can be used to obtain a better estimate for $c_e(R)$. By locating that estimate on the measured curve and reading the associated value of T, an improved estimate for R results. If $c_e(R)$ differs greatly from 0.5, it may be necessary to graphically recalculate
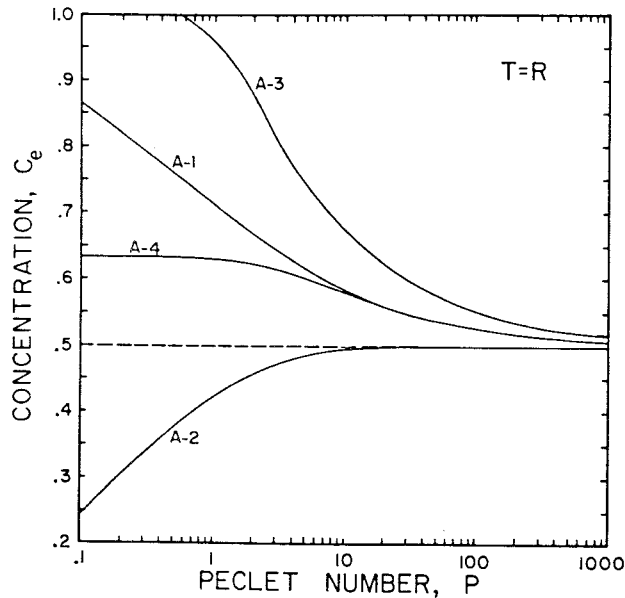
Fig. 44–6. Effect of P on the relative effluent concentration after R pore volumes ($T = R$) for the four analytical solutions of Table 44–2.

the slope S_T at $T = R$. Once improved estimates for R and S_T are available, the final value for P is obtained by again using Eq. [31].

44–5.2 Procedure

After plotting relative concentrations vs. pore volumes, $c_e(T)$, determine graphically the slope S_T of that curve at a relative concentration of 0.5. The value of T at $c_e = 0.5$ gives an initial approximation for R. Given the initial estimates for S_T and R, use Eq. [31] to obtain a first approximation for P. Use curve A-1 of Fig. 44–6 to obtain an improved estimate for the relative concentration after R pore volumes. Locate this concentration on the experimental effluent curve; the value of T at that point gives an improved estimate for R. If needed, graphically recalculate the slope S_T at the point. Application of Eq. [31] leads to an improved value for P.

44–5.3 Example

Using the tritiated water effluent curve as an example, it follows from Fig. 44–7 that the slope S_T at $c_e = 0.5$ equals $1/(1.29 - 0.65) = 1.56$, while $R = T = 0.96$ at that point. Substitution of these values into Eq. [31] yields $P = 28.2$. For this P-value, c_e at $T = R$ will be about 0.55 (curve A-1 of Fig. 44–6). The value of T at $c_e = 0.55$ in Fig. 44–7 is about 1.00, which is our improved estimate for R. Assuming that the dimensionless slope S_T of the observed curve at a relative concentration
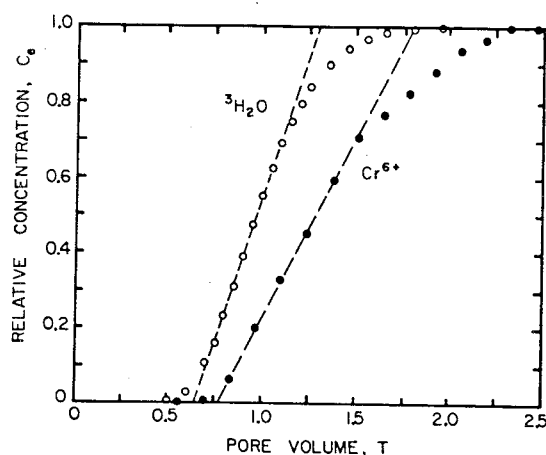
Fig. 44-7. Calculation of the dispersion coefficient from the slope of the effluent curve at $T = R$ (Method II; see text).

of 0.55 is the same as at 0.5, application of Eq. [31] with $R = 1.00$ and $S_T = 1.56$ leads to a final estimate of 30.6 for P. In actuality, the slope at $c_c = 0.55$ should be slightly smaller than at 0.5, thus causing P to be somewhat overestimated. Ignoring this small effect, we conclude that P and R are 30.6 and 1.00, respectively. Results obtained with this and the next two methods are summarized in Table 44-3. Figure 44-8 shows graphically the final results for both ^3H_2O and Cr^{6+}.

44-5.4 Comments

Method II is relatively easy to apply, requires only a minimum number of calculations, and still gives fairly accurate answers. This method is based on analytical solution A-1 of Table 44-2, and hence can be applied only to flux-averaged concentrations (effluent curves). However, for not too small values of P the method should give fairly accurate answers also for observed laboratory and field in situ measurements. Because Eq. [30] as compared to A-1 is a more accurate approximation of solution A-2 in Table 44-2, we recommend that the initial estimates for P and R be used directly in that case, i.e., without using the iteration involving curve A-1 of Fig. 44-6.

44-6 METHOD III: FROM A LOG-NORMAL PLOT OF THE EFFLUENT CURVE

44-6.1 Principles

Consider again the approximation, Eq. [30], for the relative effluent concentration. Inverting this equation yields

Table 44-3. Estimates for P and R based on several methods and for different analytical solutions. For comparison, the estimates based on Eq. [30] are also included.

| Exp. no.	Tracer	Method		Analytical solution				Eq. [30]
				A-1	A-2	A-3	A-4	
1	^3H_2O	II	P	30.6	--	--	--	28.2
			R	1.00	--	--	--	0.96
		III	P	30.3	29.9	29.4	29.2	30.7
			R	1.000	0.975	1.036	1.000	0.975
		IV	P	30.00	29.54	29.37	28.96	30.49
			R	1.000	0.967	1.035	1.000	0.968
2	Cr^{6+}	II	P	21.6	--	--	--	19.4
			R	1.34	--	--	--	1.28
		III	P	18.7	18.3	17.9	17.6	19.1
			R	1.350	1.284	1.419	1.350	1.284
		IV	P	19.65	19.19	18.95	18.59	20.11
			R	1.349	1.280	1.424	1.349	1.284
3	Cl^-	II	P	266.0	--	--	--	262.0
			R	0.92	--	--	--	0.914
		III	P	252.0	251.6	251.1	251.9	252.4
			R	0.922	0.919	0.925	0.922	0.919
		IV	P	253.6	253.1	253.1	253.0	254.1
			R	0.921	0.918	0.925	0.921	0.918
4	^3H_2O	II	P	32.4	--	--	--	30.4
			R	0.97	--	--	--	0.940
		III	P	26.8	26.4	26.0	25.7	27.1
			R	0.987	0.948	1.020	0.987	0.948
		IV	P	26.76	26.31	26.10	25.72	27.26
			R	0.973	0.937	1.012	0.973	0.938
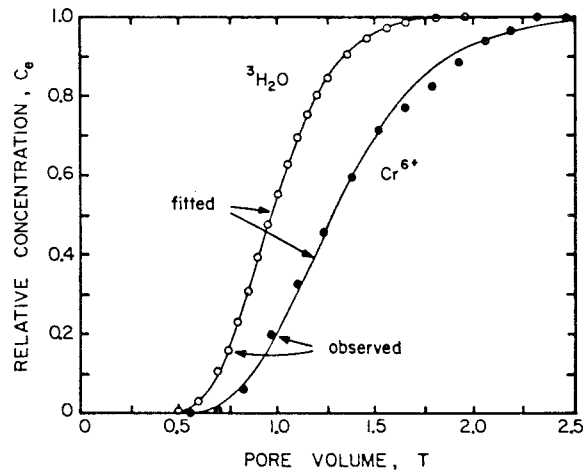
Fig. 44-8. Observed and fitted effluent curves for tritiated water and chromium (Exp. no. 1 and 2).

$$\text{inverfc}(2c_e) = (P^{1/2}/2)(1 - T/R)/(T/R)^{1/2} \qquad [32]$$

where inverfc is the inverse complementary error function. For values of y close to one, the following approximation is very accurate

$$(1 - y)/y^{1/2} \sim -\ln(y). \qquad [33]$$

Applying Eq. [33] with $y = T/R$ to Eq. [32] yields

$$\text{inverfc}(2c_e) = (P^{1/2}/2) \ln(T/R) = (P^{1/2}/2)[\ln(R) - \ln(T)]. \qquad [34]$$

This equation shows that P can be obtained from the slope of the curve inverfc($2c_e$) vs. $\ln(T)$. Calling this slope α, we have

$$P = 4\alpha^2 - \Delta \qquad [35]$$

where a correction factor Δ is introduced to account for the approximate nature of Eq. [33]. Because of this approximation, the value of Δ depends on the range of T-values used in the correlation of Eq. [35], and consequently also on the concentration range of that correlation. Equations [34] and [35] can be applied also to the four analytical solutions of Table 44-2, provided the value of Δ is properly adjusted for each case. Table 44-4 gives approximate values of Δ for the four solutions and for different concentration ranges. An alternative and more complicated expression for P as a function of α was given earlier by Rose and Passioura (1971). Their expression, which holds only for solution A-4 and for relative concentrations between 0.05 and 0.95, does not yield better results than the much simpler Eq. [35].

Once α is derived graphically from a plot of inverfc($2c_e$) vs. $\ln(T)$, the value of P is calculated with Eq. [35] using a suitable value for Δ taken from Table 44-4. R again is estimated by first using Fig. 44-6 to find $c_e(R)$ and subsequently locating that concentration on the experimental curve. The value of T associated with this point provides an estimate for R.

Table 44-4. Values for Δ in Eq. [35] associated with the four analytical solutions of Table 44-2 and for different concentration ranges.[†]

Relative concentration range	Analytical solution				
	A-1 $P > 4$	A-2 $P > 4$	A-3 $P > 9$	A-4 $P > 4$	Eq. [30] $P > 2$
0.20-0.80	0.5	0.9	1.3	1.6	0.07
0.10-0.90	0.6	1.0	1.4	1.7	0.17
0.05-0.95	0.7	1.1	1.5	1.8	0.27
0.02-0.98	0.8	1.2	1.7	1.9	0.42
0.05-0.80	0.7	1.0	1.6	1.8	0.2

† For comparison, values of Δ for approximation in Eq. [30] are also included. The values for Δ are only valid for the indicated P-values.

The method above is fairly straightforward, the main challenge being an accurate inversion of the complementary error function. One can do this by using available tables of the erfc-function (e.g., chapter 7 of Abramowitz and Stegun, 1965), or more conveniently by making use of the following inversion formula:

$$\text{inverfc}(y) = \begin{cases} f(p) & p = [-\ln(y/2)]^{1/2} & (0 < y < 1) \\ -f(p) & p = [-\ln(1 - y/2)]^{1/2} & (1 \leqslant y < 2) \end{cases} \quad [36]$$

where

$$f(p) = p - \frac{1.881796 + 0.9425908p + 0.0546028p^3}{1 + 2.356868p + 0.3087091p^2 + 0.0937563p^3 + 0.0219104p^4}.$$
$$[37]$$

This approximation, which we obtained by improving Eq. [26.2.23] of Abramowitz and Stegun (1965), has an absolute error in inverfc of less than 4.10^{-5} over the range $-4 < \text{inverfc} < 4$.

Because of the relation between the complementary error function and the normal probability function, Eq. [34] also implies that a straight line emerges when c_c is plotted vs. $\ln(T)$ on probability paper. This property obviates the need to invert erfc for each new experiment. Figure 44–9 gives an example of the type of plot that must be prepared for this purpose. The vertical axis at the left, to be identified with the observed concentrations, shows the regular probability scale between 0.0001 and 0.9999. The vertical axis on the right shows equally spaced intervals for inverfc($2c_c$). For easy reference, the plot also includes for selected values of c_c several horizontal lines exhibiting the exact values of inverfc($2c_c$). The horizontal axis of the log-normal plot (Fig. 44–9) of course must be logarithmic.

44–6.2 Procedure

Prepare a log-normal plot as shown in Fig. 44–9. If no probability paper is available, a log-normal plot can be constructed either by using published tables of the erfc-function, or by making use of Eq. [36] and [37]. Once this plot is constructed, graphically calculate the slope α of the curve inverfc($2c_c$) vs. $\ln(T)$. Use Table 44–4 to find the value of Δ applicable for a given analytical solution and a given concentration range judged to be appropriate for the analysis. Use Eq. [35] to calculate P from α and Δ. Given P, use one of the curves in Fig. 44–6 to estimate the concentration c_c after R pore volumes. Use this value of $c_c(R)$ to find $\ln(T) \equiv \ln(R)$, and hence R, from the experimental curve.
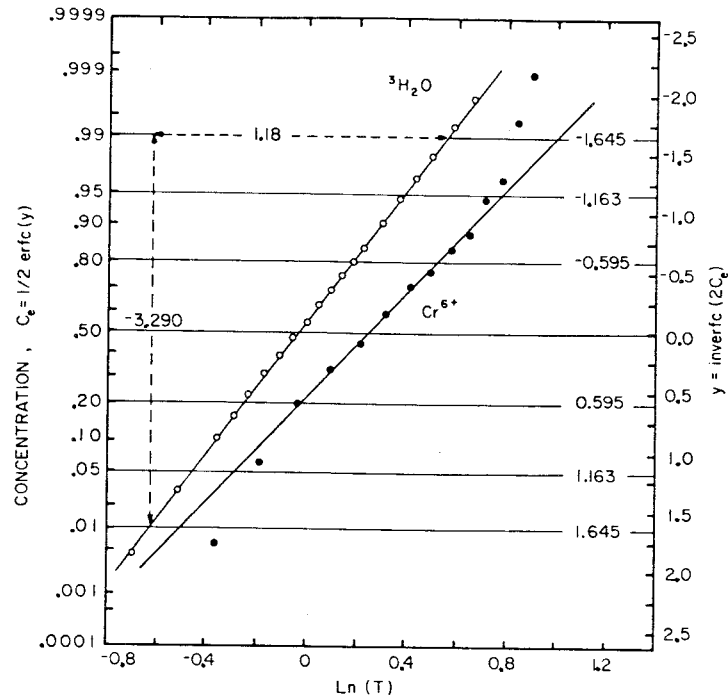
Fig. 44–9. Logarithmic-normal plots of the effluent curves shown in Fig. 44–3 (Method III).

44–6.3 Example

Figure 44–9 shows the same experimental data of Fig. 44–4 plotted vs. $\ln(T)$ on probability paper. The solid lines were eye-fitted through the data points. For the ^3H_2O curve all data points between relative concentrations of 0.02 and 0.98 were used, while for Cr^{6+} only data between 0.10 and 0.90 were considered. When drawing the curves, we recommend using more weight for observed data points close to $c_e = 0.5$; this procedure avoids too much influence being given to data points involving very low and very high concentrations (Fig. 44–9). Although deviations from the straight-line behavior at these end points of the fitted curve are important both from an experimental and conceptual point of view, these deviations are visually greatly enhanced with a probability scale. The fitted curves in Fig. 44–9 can be obtained also by applying least-squares techniques (Rose & Passioura, 1971; Passioura et al., 1970). Unfortunately, such an approach again will put too much emphasis on the extreme low and high concentrations.

The slope α of the ^3H_2O-curve (see Fig. 44–9) equals $(-1.18/3.29)$ or 2.79. Equation [35] with $\Delta = 0.8$ (Case A-1 of Table 44–3) gives $P = 30.3$. The relative concentration after R pore volumes for this P-value is about 0.54 (Fig. 44–6), which leads to an estimate of 0.0 for $\ln(R)$. Hence $R = 1.00$. Estimates of P and R for solution A-1 and the other three analytical solutions are listed in Table 44–3.

The procedure for chromium is exactly the same. The slope α is determined graphically from Fig. 44–6: $\alpha \sim 2.326/1.06 = 2.194$. With $\Delta = 0.6$ (Case A-1 for the concentration range 0.1 to 0.9 in Table 44–4), this leads to $P = 18.7$. Since $c_c = 0.56$ at $T = R$ for this P-value (Fig. 44–6), it follows from Fig. 44–9 that $\ln(T)$ is about 0.30. This in turn gives $R = 1.35$ for the chromium curve.

44–6.4 Comments

While a log-normal plot of experimental data is not expected to yield exactly a straight line because of the approximations discussed above, deviations of the magnitude of those shown for the chromium curve in Fig. 44–6 cannot be explained on that basis. Several situations will lead to these types of deviations, such as the use of undisturbed, aggregated, or otherwise structured soils, soils containing large macropores that induce preferential solute transport, channeling of water along the walls of a poorly packed soil column during saturated flow, or fingering caused by density differences between the displacing and displaced solution. Also chemical effects, such as nonlinear adsorption or cation exchange in general, can lead to serious deviations from the log-normal distribution. Figure 44–10 shows two additional experimental curves, one for chloride transport through a loam soil that yields a straight line and one for tritiated water movement through an aggregated clay loam that quite severely deviates from the straight log-normal line. Analysis of the chloride data is straightforward, yielding P and R-values as shown in Table 44–3. Unfortunately, some judgment is needed when analyzing the ^3H_2O curve. In this case, a straight line was drawn through the data points located between relative concentrations of 0.2 and 0.8. The fitted effluent curves for Cl and ^3H_2O are both shown in Fig. 44–11. Note that the observed tritiated water curve deviates considerably from the straight log-normal plot in Fig. 44–10, but that the fitted curve in Fig. 44–11 is still quite reasonable; serious deviations occur only at the higher concentrations. The fitted curve in this case was based on analytical solution A-2 (Table 44–2). The other solutions generated essentially the same fitted curve, albeit with slightly different values for P and R (Table 44–3).

Method III involves a few more calculations than the somewhat simpler Method II, notably the cumbersome inversion of the complementary error function. Fortunately, the number of calculations can be reduced drastically by first preparing special logarithmic-normal paper as shown in Fig. 44–6. Once this special paper is available, the analysis can be carried out quickly and easily. Results obtained with Method III are generally more accurate than those based on Method II. This is a direct consequence of the fact that the slope S_T for Method II must be determined after exactly R pore volumes. Because this slope changes from point to point on the curve, its value is not easy to pinpoint exactly and in a reproducible manner. On the other hand, the approximately straight log-normal plot of Method III allows a much broader concentration range
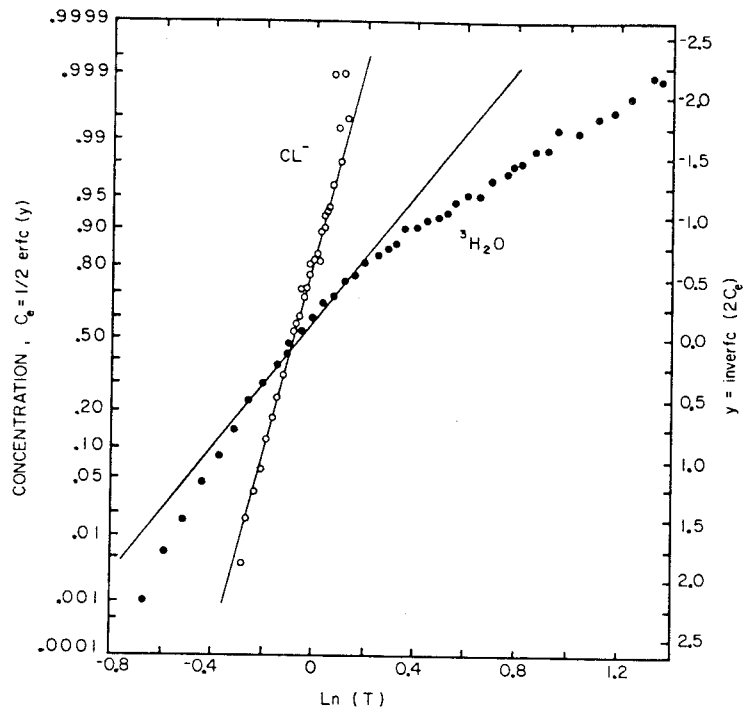
Fig. 44–10. Logarithmic-normal plots of effluent curves for Exp. no. 3 and 4 (Table 44–3).
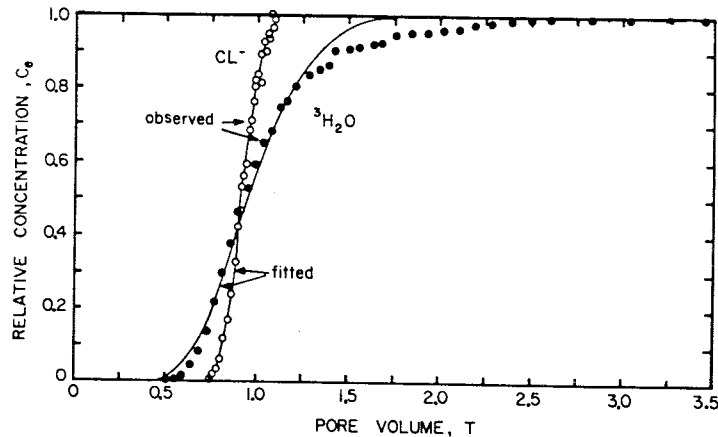
Fig. 44–11. Observed and fitted effluent curves for Exp. no. 3 and 4 (Method III).

to be used when determining the slope α, which in turn will lead to a more accurate estimate for P. An additional advantage of Method III is its applicability to all four analytical solutions, whereas Method II holds only for solution A-1. A disadvantage of Method III is that results based on this method can become quite inaccurate when P becomes less than about 5 (see Table 44–4).

44-7 METHOD IV: LEAST-SQUARES ANALYSIS OF THE EFFLUENT CURVE

44-7.1 Principles

The trial-and-error method discussed earlier (Method I) is based on a series of comparisons between observed and calculated effluent curves until a satisfactory visual fit of the observed curve is obtained. This method can be expanded into a more formal approach by continuously adjusting P and R until a least-squares fit of the observed data is obtained. This is done by minimizing the residual sum of squares (R_s)

$$R_s = \sum_{i=1}^{n} \left[c_e(L, T_i) - c(L, T_i) \right]^2 \qquad [38]$$

where $c_e(L,T_i)$ and $c(L,T_i)$ are the observed and calculated data points at pore volume T_i, and n is the number of observed data points. Several methods for minimizing R_s are available, ranging from relatively simple graphical methods to computerized solutions using existing least-squares inversion methods (Elprince & Day, 1977; Laudelout & Dufey, 1977; Le Renard, 1979; van Genuchten, 1980, 1981; Parker & van Genuchten, 1984b). Table 44-3 gives for all four experiments the fitted values of P and R as obtained with the least-squares program of van Genuchten (1980). This program is available upon request from the senior author.

44-7.2 Comments

Results based on least-squares optimization methods are the most accurate, are valid for all values of P and R, and are reproducible on different occasions and by different investigators. Once programmed, computerized least-squares methods are also by far the most convenient ones to use. In addition, they can be extended easily to situations where pulse-type effluent curves are present, i.e., to cases where the tracer is in the feed solution for only a relatively short period of time. Parker and van Genuchten (1984b) recently published a least-squares optimization method that can be used to estimate D and R from observed breakthrough data obtained at more than one distance from the soil surface. Clearly, such an approach extracts the most information from available experimental data.

44-8 METHOD V: FROM CONCENTRATION-DISTANCE CURVES

In some cases dispersion coefficients must be estimated from concentration-distance curves. Such curves can be obtained by sectioning laboratory soil columns or by determining solute concentration in situ,

either in laboratory soil columns or in field soils. Two methods for these situations are discussed briefly below. Both methods are based on Eq. [28], and consequently, can yield only approximate estimates for D and R. Not mentioned any more are trial-and-error and least-squares methods; application of these methods to concentration-distance curves is, at least in principle, straightforward. For the documentation of a least-squares optimization program applicable to concentration distributions vs. distance, see Parker and van Genuchten (1984b).

Differentiating Eq. [28] with respect to x and evaluating the resulting expression at $Rx = vt$ leads to the following equation for D:

$$D = R/4\pi t\, S_x^2 \qquad\qquad [39]$$

where S_x is the slope of the experimental curve at $c = 0.5$. Since at this point $Rx = vt$, Eq. [39] can be written also in the form

$$D = v/4\pi x_o\, S_x^2 \qquad\qquad [40]$$

where x_o is the value of x where the relative concentration attains a value of 0.5. Equations [39] and [40] are evaluated in a similar way as Eq. [31] for Method II. Contrary to Method II, however, the present equations are applicable only to Eq. [28]. Hence, they cannot be applied to any of the analytical solutions in Table 44–1.

A procedure somewhat similar to Method III follows by inverting Eq. [28]:

$$\mathrm{inverfc}(2c) = (Rx - vt)/2(DRt)^{1/2}. \qquad\qquad [41]$$

This equation shows that D can be obtained also from the slope, β, of the curve $\mathrm{inverfc}(2c)$ vs. x. The predictive equation for D in this case is

$$D = R/4\beta^2 t \qquad (R = vt/x_o). \qquad\qquad [42]$$

44–9 OTHER TRANSPORT MODELS

The different methods described above all deal with transport Eq. [11], a model that considers linear equilibrium adsorption but ignores production or decay. For many organics, N species, or radionuclides, additional terms are usually needed that describe zero- and/or first-order production or decay processes. A general transport model for that case is

$$R\frac{\partial C}{\partial t} = D\frac{\partial^2 C}{\partial x^2} - v\frac{\partial C}{\partial x} - \mu C + \gamma \qquad\qquad [43]$$

where μ and γ are first- and zero-order rate coefficients. Because of the production and decay terms, simple methods analogous to Methods II, III, and V are not available for estimating D, R, μ, and/or γ. However, an easy-to-use computer program that couples a least-squares optimization method with various analytical solutions of Eq. [43] recently has been made available by Parker and van Genuchten (1984b). Their program can be applied to observed concentration distributions vs. time and/or distance.

Least-squares computerized methods can be conveniently used also to estimate parameters that appear in more complicated transport models. For example, van Genuchten (1981) published a program that is applicable to various physical and chemical nonequilibrium models. His program is limited to breakthrough curves in time. The program of Parker and van Genuchten (1984b) considers similar nonequilibrium models applicable to concentration-distance curves as well.

44-10   GENERAL COMMENTS

As outlined above, several methods are available for determining D (or P) and R. The two simplest methods (I and II) are probably most appropriate when the effluent curve is poorly defined. This may be due to a limited number of (inaccurate) data, considerable scatter between the data points, or serious deviations from the mostly sigmoidal-type curves shown in this study. Methods based on least-squares techniques or on log-normal plots of the data are best reserved for cases where the experimental curve is well-defined. Of all existing methods, least-squares computer methods are the most accurate and at the same time the most convenient ones to use. Provided that the necessary computer facilities are available, we strongly recommend their use.

As was pointed out already in section 44-2, we emphasize again that the fitted values of D and R ultimately are associated with one of the analytical solutions in Table 44-1. Methods based on different analytical solutions but applied to the same experimental data will lead to different values for D and R. These differences can become especially noticeable for relatively small values of the dimensionless group (vx/D), or in the case of effluent curves of the column Peclet number, P. Figure 44-1 suggests that for P-values greater than about 20, the fitted value of the dispersion coefficient becomes more or less independent of the method used to determine that value. In practice, this means that experiments should be carried out on columns of at least 10 to 15 cm length in case of homogeneous soils with relatively narrow pore-size distributions, and on columns of at least 30 to 50 cm length if undisturbed, aggregated, or other soils are present that have a relatively broad pore-size distribution. If column experiments are used primarily to determine the retardation factor, R (or the linearized distribution coefficient, k), then a shorter

column is allowed, provided that only methods based on analytical solutions A-1 or A-4 of Table 44–2 are used.

44–11 APPENDIX

Data for four column displacement experiments.

Example	1		2		3		4	
Tracer:	^3H_2O		Cr^{6+}		Cl^-		^3H_2O	
θ (cm^3 cm^{-3})	0.400		0.184		0.363		0.453	
ϱ (g cm^{-3})	1.400		1.68		1.53		1.22	
q (cm day^{-1})	10.0		3.61		5.16		17.0	
L (cm)	30.0		5.0		30.0		30.0	
	T	c_e	T	c_e	T	c_e	T	c_e
	0.50	0.0042	0.558	0.000	0.749	0.004	0.512	0.001
	0.60	0.0294	0.695	0.006	0.768	0.017	0.556	0.006
	0.70	0.1015	0.831	0.061	0.787	0.035	0.599	0.016
	0.75	0.1586	0.967	0.198	0.806	0.059	0.643	0.045
	0.80	0.2279	1.103	0.325	0.825	0.114	0.686	0.082
	0.85	0.3057	1.236	0.450	0.845	0.169	0.730	0.138
	0.90	0.3881	1.375	0.592	0.864	0.240	0.774	0.216
	0.95	0.4709	1.511	0.705	0.883	0.326	0.817	0.296
	1.00	0.5507	1.647	0.768	0.902	0.421	0.861	0.376
	1.05	0.6247	1.783	0.841	0.911	0.467	0.904	0.465
	1.10	0.6913	1.919	0.881	0.921	0.531	0.948	0.529
	1.15	0.7497	2.055	0.944	0.930	0.562	0.992	0.593
	1.20	0.7996	2.191	0.966	0.940	0.594	1.035	0.655
	1.25	0.8414	2.327	0.994	0.949	0.709	1.079	0.685
	1.35	0.9037	2.463	0.999	0.959	0.688	1.122	0.745
	1.45	0.9436			0.968	0.712	1.166	0.764
	1.55	0.9679			0.978	0.767	1.218	0.806
	1.65	0.9822			0.987	0.806	1.284	0.834
	1.80	0.9929			0.997	0.822	1.340	0.850
	1.95	0.9973			1.006	0.838	1.384	0.866
					1.016	0.814	1.428	0.901
					1.025	0.893	1.501	0.905
					1.035	0.900	1.558	0.915
					1.044	0.924	1.646	0.923
					1.054	0.935	1.689	0.928
					1.063	0.940	1.754	0.947
					1.073	0.963	1.848	0.953
					1.082	0.999	1.935	0.953
					1.092	0.993	2.022	0.968
							2.110	0.974
							2.196	0.979
							2.283	0.981
							2.392	0.986
							2.517	0.987
							2.608	0.993
							2.824	0.994
							3.040	0.995
							3.257	0.996
							3.473	0.998

44-12 REFERENCES

Abramowitz, M., and I. A. Stegun. 1965. Handbook of mathematical functions. Fourth printing. Applied Math. Ser. 55, U. S. Government Printing Office, Washington, DC.

Agneessens, J. P., P. Dreze, and L. Sine. 1978. Modélisation de la migration d'éléments dans les sols. II. Détermination du coefficient de dispersion et de la porosité efficace. Pedologie 27:373–388.

Aris, R. 1958. On the dispersion of linear kinematic waves. Proc. R. Soc. London, Ser. A 245:268–277.

Bear, J. 1972. Dynamics of fluids in porous media. American Elsevier Publishing Co., New York.

Boast, C. W. 1973. Modeling the movement of chemicals in soils by water. Soil Sci. 115:224–230.

Brenner, H. 1962. The diffusion model of longitudinal mixing in beds of finite length. Numerical values. Chem. Eng. Sci. 17:229–243.

Brigham, W. E. 1974. Mixing equations in short laboratory cores. Soc. Pet. Eng. J. 14:91–99.

Cleary, R. W., and D. D. Adrian. 1973. Analytical solution of the convective-dispersive equation for cation adsorption in soils. Soil Sci. Soc. Am. Proc. 37:197–199.

Danckwerts, P. V. 1953. Continuous flow systems. Chem. Eng. Sci. 2:1–13.

Elprince, A. M., and P. R. Day. 1977. Fitting solute breakthrough equations to data using two adjustable parameters. Soil Sci. Soc. Am. J. 41:39–41.

Freeze, R. A., and J. A. Cherry. 1979. Groundwater. Prentice Hall, Englewood Cliffs, NJ.

Fried, J. J., and M. A. Combarnous. 1971. Dispersion in porous media. Adv. Hydrosci. 7:169–282.

Gaudet, J. P., H. Jegat, G. Vachaud, and P. J. Wierenga. 1977. Solute transfer, with exchange between mobile and stagnant water, through unsaturated sand. Soil Sci. Soc. Am. J. 41:665–671.

Hillel, D. 1980. Fundamentals of soil physics. Academic Press, New York.

Jury, W. A., and G. Sposito. 1985. Field calibration and validation of solute transport models for the unsaturated zone. Soil Sci. Soc. Am. J. 49:1331–1341.

Kirkham, D., and W. L. Powers. 1972. Advanced soil physics. Wiley-Interscience, New York.

Kreft, A., and A. Zuber. 1978. On the physical meaning of the dispersion equation and its solutions for different initial and boundary conditions. Chem. Eng. Sci. 33:1471–1480.

Lapidus, L., and N. R. Amundson. 1952. Mathematics of adsorption in beds. IV. The effect of longitudinal diffusion in ion exchange chromatographic columns. J. Phys. Chem. 56:984–988.

Laudelout, H., and J. E. Dufey. 1977. Analyse numérique des expériences de lixiviation en sol homogène. Ann. Agron. 28:65–73.

Le Renard, J. 1979. Description d'une méthode de détermination du coefficient de dispersion hydrodynamique longitudinal en milieu poreux homogène saturé en eau. II. Utilisation d'un modèle mathematique a trois paramètres dont un phénomenologique. Ann. Agron. 30:109–119.

Lindstrom, F. T., R. Hague, V. H. Freed, and L. Boersma. 1967. Theory on the movement of some herbicides in soils: linear diffusion and convection of chemicals in soils. Environ. Sci. Technol. 1:561–565.

Nielsen, D. R., and J. W. Biggar. 1961. Miscible displacement in soils: I. Experimental information. Soil Sci. Soc. Am. Proc. 25:1–5.

Nielsen, D. R., R. D. Jackson, J. W. Cary, and D. D. Evans (ed.) 1972. Soil water. American Society of Agronomy and Soil Science Society of America, Madison, WI.

Parker, J. C., and M. Th. van Genuchten. 1984a. Flux-averaged and volume-averaged concentrations in continuum approaches to solute transport. Water Resour. Res. 20:866–872.

Parker, J. C., and M. Th. van Genuchten. 1984b. Determining transport parameters from laboratory and field tracer experiments. Virginia Agric. Exp. Stn. Bull. 84.

Passioura, J. B., D. A. Rose, and K. Haszler. 1970. Lognorm: a program for analysing experiments on hydrodynamic dispersion. Tech. Memorandum 70/6. CSIRO, Div. of Land Res., Canberra, Australia.

Rifai, M. N. E., W. J. Kaufman, and D. K. Todd. 1956. Dispersion phenomena in laminar flow through porous media. Sanitary Eng. Res. Lab., Univ. of California, Berkeley. Inst. Eng. Res. Ser. no. 93(2).

Rose, D. A., and J. B. Passioura. 1971. The analysis of experiments on hydrodynamic dispersion. Soil Sci. 111:252–257.

Saxena, S. K., F. T. Lindstrom, and L. Boersma. 1974. Experimental evaluation of chemical transport in water-saturated porous media: 1. Nonsorbing media. Soil Sci. 118:120–126.

Shamir, U. Y., and D. R. F. Harleman. 1966. Numerical and analytical solutions of dispersion problems in homogeneous and layered aquifers. Rep. no. 89. Hydrodynamics Lab. Dep. of Civil Engineering, Massachusetts Institute of Technology.

Skopp, J. 1985. Analysis of solute movement in structured soils. p. 220–228. In J. Bouma and P.A.C. Raats (ed.) Proc. ISSS Symp. Water and Solute Movement in Heavy Clay Soils. International Institute for Land Reclamation and Improvement, Wageningen, Netherlands.

Valocchi, A. J. 1985. Validity of the local equilibrium assumption for modeling sorbing solute transport through homogeneous soils. Water Resour. Res. 21:808–820.

van Genuchten, M. Th. 1980. Determining transport parameters from solute displacement experiments. Res. Rep. 118. U.S. Salinity Lab., Riverside, CA.

van Genuchten, M. Th. 1981. Non-equilibrium transport parameters from miscible displacement experiments. Res. Rep. 119. U. S. Salinity Lab., Riverside, CA.

van Genuchten, M. Th., and W. J. Alves. 1982. Analytical solutions of the one-dimensional convective-dispersive solute transport equation. USDA-ARS Tech. Bull. 1661. U.S. Government Printing Office, Washington, DC.

van Genuchten, M. Th., and J. C. Parker. 1984. Boundary conditions for displacement experiments through short laboratory soil columns. Soil Sci. Soc. Am. J. 48:703–708.

Wierenga, P. J., R. J. Black, and P. Manz. 1973. A multichannel syringe pump for steady state flow in soil columns. Soil Sci. Soc. Am. Proc. 37:133–134.

Wierenga, P. J., M. Th. van Genuchten, and F. W. Boyle. 1975. Transfer of boron and tritiated water through sandstone. J. Environ. Qual. 4:83–87.

Yu, C., W. A. Yester, and A. R. Jarrett. 1984. Simultaneous determination of dispersion coefficients and retardation factors for a low level radioactive waste burial site. Radioact. Waste Manage. Nucl. Fuel Cycle 4:401–420.